

RECONSTRUCTION OF SEVERAL LANDSLIDE DAMMED LAKES IN THE UPPER REACHES OF JINSHA RIVER AND ITS INFLUENCE ON RIVER PROFILE EASTERN TIBETAN PLATEAU

LiQin Zhou^{1,2}, Lu Cong^{3*}

¹State Key Laboratory of Mountain Hazards and Engineering Resilience, Institute of Mountain Hazards and Environment, Chinese Academy of Sciences, Chengdu 610299, Sichuan, China.

²University of Chinese Academy of Sciences, Beijing 100049, China.

³Chengdu Academy of Educational Sciences (Chengdu Research Office of Basic Education), Chengdu 610036, Sichuan, China.

Corresponding Author: Lu Cong, Email: cong_lu@yeah.net

Abstract: The damming phenomenon caused by landslides is a significant disturbance factor in the evolution of mountainous rivers, influencing river morphology across multiple timescales. The temporal characteristics of this phenomenon are often analyzed by examining the relationship between dam locations and the river longitudinal profile within a specific area. In the Batang section of the upper Jinsha River, located within the Jinsha river suture zone, intense tectonic activity makes the region highly susceptible to geological hazards such as landslides. Through data collection, remote sensing interpretation, and field investigations, we identified nine landslide dams in this area. Systematic studies of these dams were conducted, including preliminary measurements of dam heights and volumes. By reconstructing dam elevations, we calculated the areas, volumes, and peak discharge flows of the associated dammed lakes. A detailed analysis of the Wangdalong landslide dam revealed that its maximum lake surface area reached 106.70 million m², with a maximum volume of 14.57 billion m³. The peak discharge flow was calculated at 31.98×10^4 m³/s, and the dammed lake existed for a duration of approximately 1.09-1.76 ka. Additionally, a comparison of river geomorphological parameters indicated that the impact of a single dammed lake on the river's longitudinal profile is limited when its duration is relatively short. However, clusters of dammed barriers significantly affect the river steepness index, increasing the likelihood of forming knickpoints. These findings provide valuable insights into the role of landslide dams in shaping the geomorphological evolution of mountainous river systems.

Keywords: Landslide dammed lake; River profile; Luminescence dating; Jinsha River

1 INTRODUCTION

Landslide-induced river blockages represent a prevalent geohazard in mountainous terrain with steep topography and confined valleys. Even moderate slope failures can trigger cascading disasters through valley obstruction, subsequent lake formation, and catastrophic dam breaches, posing substantial risks to downstream communities. Particularly along the tectonically active Jinsha River on the Tibetan Plateau margin, recurrent damming events are facilitated by intense fluvial incision and neotectonic deformation [1]. The 2018 Baige landslides exemplify modern catastrophic damming incidents, generating two sequential barrier lakes and destructive outburst floods [2]. The resulting upstream inundation and downstream outburst floods caused extensive damage to infrastructure, including residential areas, bridges, and roadbeds along National Highway 318, underscoring the significant hazards associated with such events.

Landslide-dammed lakes represent a prevalent geological phenomenon in mountainous regions, arising from the interplay of topography, climatic conditions, and tectonic activities [3-5]. The vestiges of such events—including fluvial erosion traces and lacustrine sediments on riverbanks—serve as critical evidentiary markers for reconstructing and identifying historical river-blocking incidents [6]. By analyzing the elevation of lacustrine deposits, paleo-dammed lake water levels can be estimated, while the integration of geomorphic datasets enables the reconstruction of lake areal extent and storage capacity [7,8]. On geological timescales, landslide-induced river blockages and subsequent outburst flood events exert significant influences on fluvial geomorphology through modifications to sediment transport fluxes [9]. Recent research has demonstrated that such dams profoundly alter river longitudinal profiles, thereby complicating the interpretation of tectonic activities and reshaping the understanding of regional geomorphological evolution [1,10].

The upper Jinsha River in the Hengduan Mountain Range exhibits intense tectonic activity and steep topography, predisposing it to recurrent river-blocking landslides. While previous studies have reconstructed individual paleo-damming events and analyzed lacustrine sediments [11-14], key gaps remain in understanding their geomorphic impacts [7], particularly on longitudinal river profiles and quantitative landscape evolution. This study focuses on the Batang reach, a hotspot for paleo-landslide dams, employing field surveys, OSL dating, and digital topographic analysis to characterize dam structures, reconstruct reservoir capacities, and establish event chronologies. By evaluating the influence of these dams on river morphology, the research advances insights into landslide-fluvial interactions in tectonically active settings.

2 REGIONAL SETTING

The study area is situated in the northern Hengduan Mountains section of the upper Jinsha River on the southeastern margin of the Tibetan Plateau, within the Jinshajiang suture zone (Figure 1). Influenced by the rapid uplift of the Tibetan Plateau and intense fluvial incision, steep canyon landforms dominate the region [6]. Tectonic activity is pronounced, with major active faults such as the Batang Fault and Xiongsong-Suwalong Fault. Since 1722, seven earthquakes of magnitude ≥ 6 have been recorded, reflecting frequent geohazards [15]. The lithology is complex (Figure 2), primarily comprising Permian schists, basic volcanic rocks, crystalline limestones, Triassic siltstones, intermediate-basic volcanic rocks, hercynian medium-coarse diorites, and indosinian biotite granites.

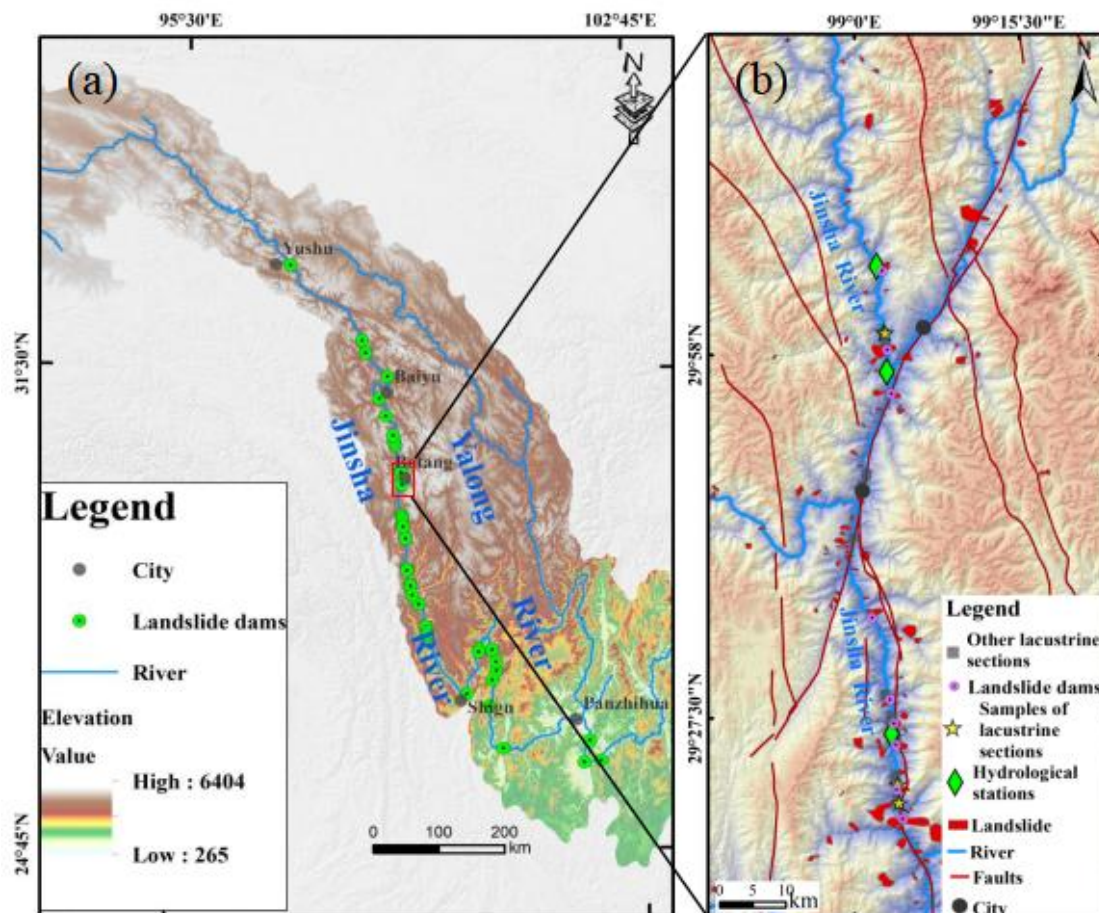


Figure 1 Geological Map of Batang Section of the Upper Jinsha River

The area experiences a dry-hot valley climate, with an average annual precipitation of 480.4 mm (94% concentrated between May and October). Sparse vegetation and intense physical weathering prevail. Quaternary deposits are dominated by fluvial and slope sediments, including low-liquid-limit clays, gravelly soils, and sand-cobble accumulations along riverbanks. Lacustrine sediments, primarily distributed in riverbeds and localized bank sections, serve as critical evidence for identifying paleo-damming events. Fine-grained lacustrine deposits (e.g., clays and silts) formed during stable lake phases contrast markedly with coarse-grained fluvial deposits (e.g., gravels and well-rounded pebbles).

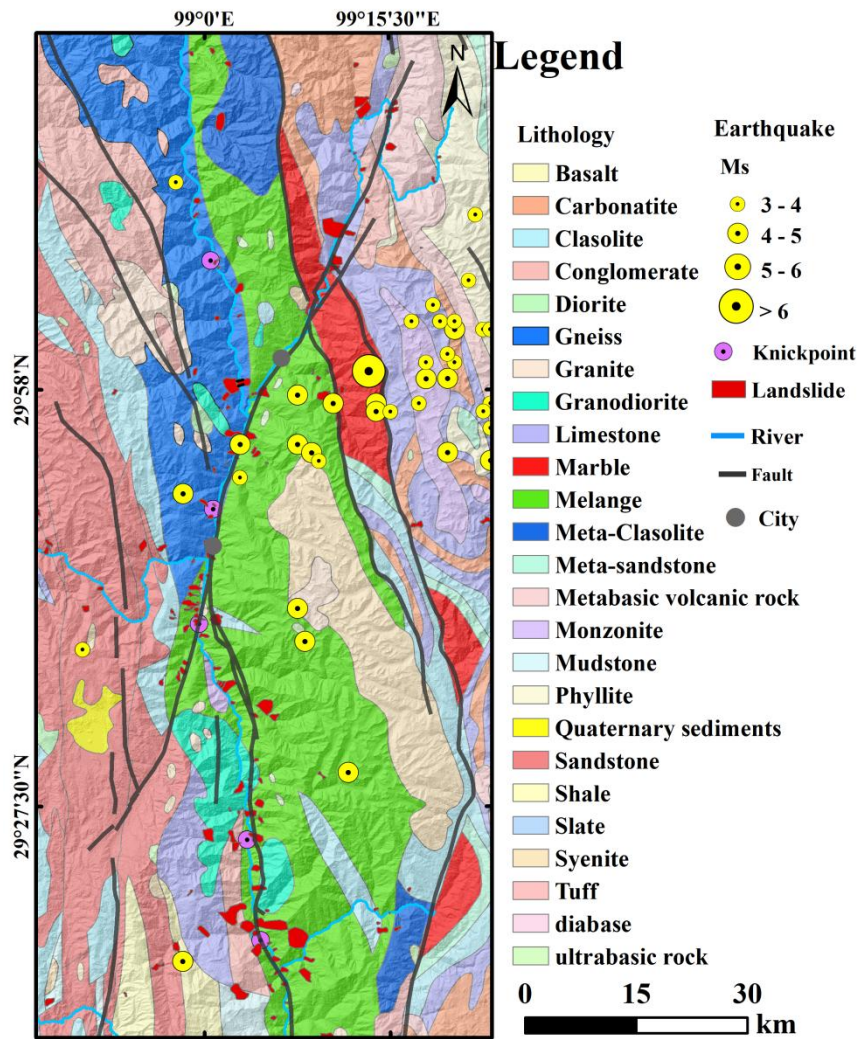


Figure 2 Geological Map of Batang Section of the Upper Jinsha River

3 MATERIALS AND METHODS

3.1 Geomorphic Field Work and Sampling

First, through remote sensing interpretation and data collection, we obtained the location of some landslides in the Batang section of the main stream of the Jinsha River. Then the field survey along the Jinsha River to verify the accuracy of the remote sensing interpretation results. Through the investigation of the residual dam body accumulation and the lacustrine sediment, the exact position of the landslide dam is finally obtained. At the same time, we also sampled some of the lacustrine deposits for dating testing. We mapped the position, altitude, relative elevation to river levels using a laser TruPulse 200 range finder and handheld Trimble Juno 3B GPS (global positioning system). We obtained the height of the dam by the difference between the elevation of the dam outburst and the channel (Figure 3). Using field results, we delineated the extent of the landslide relict dam on DEM and Google Earth, estimates the area of the dam, and then uses the landslide volume and area relationship derived [16]:

$$V = \alpha A^\gamma \quad (1)$$

Where V is the volume (m^3), A is the area (m^2), and α and γ are power-law scaling parameters, the $\alpha=0.23$ and $\gamma=1.41$ is used to estimate the volume of the landslide dam [7,16].

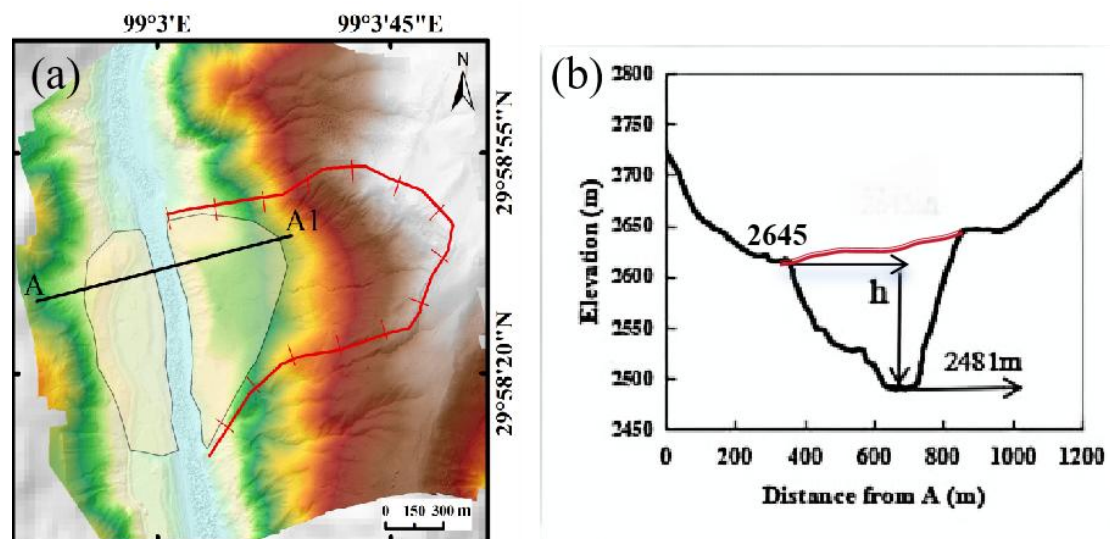


Figure 3 Range and Height of Temi Landslide Dam. (a) Range of Relict Dam of Temi Landslide (b) Line Graphs of Cross-Section AA1, h is Dam Height

3.2 Optically-stimulated luminescence dating

Ten samples were collected from four lacustrine sections for optically stimulated luminescence (OSL) dating to estimate the chronological limits of the studied dammed lake events. The chemical extraction of pure quartz grains from sediment and OSL measurements, which performed under subdued red light, based on the pretreatment steps and measurement procedure reported in Lai and Ou (2013) [17]. All the processes were completed in the OSL laboratory of the Qinghai Institute of Salt Lakes, Chinese Academy of Sciences, which is equipped with a RisøTL/OSL-DA-20 reader. In this study, we applied a combination of the single-aliquot regenerative-dose (SAR) protocol [18,19] and the standard growth curve (SGC) method [20] to determine the equivalent dose (D_e) values of samples. The optical measurements were performed after heating at a temperature of 260 °C for 10 s for natural and regenerative doses, and after preheating at a temperature 220 °C for 10 s for test doses. For 38-63 μm grains, the α efficiency value of 0.035 ± 0.003 was adopted during dose rate calculation [21]. The U, Th contents were measured using ICP-MS, and the K content was measured using ICP-OES in the Qinghai Institute of Salt Lakes, Chinese Academy of Sciences. And we used water content of $15 \pm 5\%$ to calculate dose rate calculations for lacustrine samples based on data on moisture content and modern annual precipitation [7,19]. The cosmic ray contribution was determined based on the burial depth and the geomagnetic coordinate of the research sites [22].

3.3 Digital Terrain Analysis

The 30 m SRTM DEM data used in this paper are all obtained from the US Geological Survey United States Geological Survey (USGS) data sharing platform (<https://earthexplorer.usgs.gov/>). In this paper, the TopoToolbox was used to extract the river geomorphic parameters [23], and the TopoToolbox to extract the DEM containing projection information as the input data (<https://topotoolbox.wordpress.com/>). Considering the geographical location of the Jinsha river, the projection coordinate system used in this study is WGS_1984_UTM_zone_47_N. To learn more about the effect of the landslide dam on the river channel, the channel width was measured using Google Earth images, the channel width selected is the modern wetted-width calculated every kilometer over 160 km.

To obtain the effect of the landslide dam on the river longitudinal profile in the Jinsha River, we used the Stream-Power River Incision Model, it can be quantified by relationship between upstream catchment area and channel gradient [24]:

$$S = k_s A^{-\theta} \quad (2)$$

where S is channel slope, k_s is the steepness index, A is the upstream catchment area. In this study we fixed concavity index of $\theta = 0.45$ to extract the normalized steepness index (k_{sn}) to facilitate the comparison of the differences between of more reaches [25]. In here, the value of k_{sn} was calculated by the algorithms in TopoToolbox with $K=5$ and $\tau=0.5$, which is software for the analysis of DEMs [26]. In addition, We also applied the KnickpointFinder function in TopoToolbox, which reproducibly extracts knickpoint locations from smooth river profiles, over the whole river network [23,26].

4 RESULTS

4.1 Characteristics of Landslide Dam

By remote sensing interpretation and field investigation, we found nine landslide dams in the Batang section of Jinsha River, From upstream to downstream is the lawa landslide dam, Temi landslide dam, Niuying landslide dam, Xiaguiwa landslide dam, Xuelongnang landslide dam, Suoduoxi landslide dam, Suwalong landslide dam, Biji landslide dam,

Wangdalong landslide dam (Figure 4). At the same time, we also found a total of 18 lacustrine sediments sections upstream of the landslide dam, but not all of the upstream dam retained lacustrine deposits. These lacustrine deposits are mainly distributed in upstream of Temi landslide dam, Xuelongnang landslide dam, Suoduoxi landslide dam, Suwalong landslide dam, Biji landslide dam, Wangdalong landslide. At the same time, we determined the area and height of the dam according to the position and elevation of the residual dam body, and then estimated the volume of the 9 landslide dams using the classical formula of area and volume [16]. The parameters of the landslide dam obtained are shown in Table 1, among them, the volume and height of the dam of Wangdalong landslide dam are the largest.



Figure 4 Nine Damming Landslides in the Upper Reaches of Jinsha River. (a) Lawa Landslide; (b) Temi Landslide; (c) Niuying Landslide; (d) Xiawagui Landslide; (e) Xuelongnang Landslide; (f) Suoduoxi Landslide; (g) Suwalong Landslide; (h) Biji Landslide; (i) Wangdalong Landslide. Image Credit: Google Earth

Table 1 Scale Statistics of Landslide Dams

Name	Longitude (N)	Latitude (E)	Dam area (10^4m^2)	Dam height (m)	Dam volume (10^6m^3)
Lawa landslide	30° 5'4.44"	99° 2'35.16"	39.18	46	17.70
Temi landslide	29°58'25.50"	99° 3'3.01"	94.70	164	61.43
Niuying landslide	29°54'46.66"	99° 3'23.11"	92.83	46	59.72
Xiaguiwa landslide	29°35'58.15"	99° 1'38.05"	61.45	134	33.38
Xuelongnang landslide	29°29'5.58"	99° 3'18.86"	91.64	87	58.65
Suoduoxi landslide	29°27'5.33"	99° 3'40.81"	90.53	90	57.65
Suwalong landslide	29°25'27.65"	99° 3'57.76"	65.96	78	36.89
Biji landslide	29°21'33.24"	99° 3'56.00"	51.62	100	26.11
Wangdalong landslide	29°19'5.90"	99° 4'30.05"	224.75	316	207.78

4.2 OSL Dating Results

We selected 10 OSL samples from two lacustrine deposits sections (BT-1, BT-2) in upstream of Temi landslide dam

(Figure 5a, 5b), one lacustrine deposits section (BT-3) in upstream of Biji landslide dam (Figure 5c) and one lacustrine deposits section (BT-4) in upstream of WangDalong landslide dam (Figure 5d), the OSL dates for lacustrine sediments are summarized in Table 2. The BT-1 section height is approximately 11 m thick, the elevation is 2521 m, consists of silty clay varves. The BT-2 section height is approximately 1 m thick, the elevation is 2535 m, consists of climbing ripples of silt and clay vares, it belongs to the shallow lacustrine deposit. The BT-3 section height is about 5 m thick, the elevation is 2445 m, consists of Planar and parallel laminations lacustrine clay varves. The BT-4 section height is about 22.3 m thick, the elevation is 2391m, the upper 3.4-m-thick part contains fluvial gravel layer. The middle part, which is 6.7-m-thick, consists of wavy lamination and typical lacustrine silt and clay varves. The lower part, which is about 13-m-thick, consists of contains climbing ripples of fine sand and silt, and the lamination is slightly wavy. A preliminary analysis of the results of the dating of the lake sediments in Table 2, we found that the dating results of these lacustrine section tended to be consistent and fit to the formation order, except for JSJ 23-26 sample. Further research found that there were more roots near the sample, which may have affected his chronological results. The bottom age of the four lake facies was mainly about 1.7 ka, while the top age of the lake facies was different.

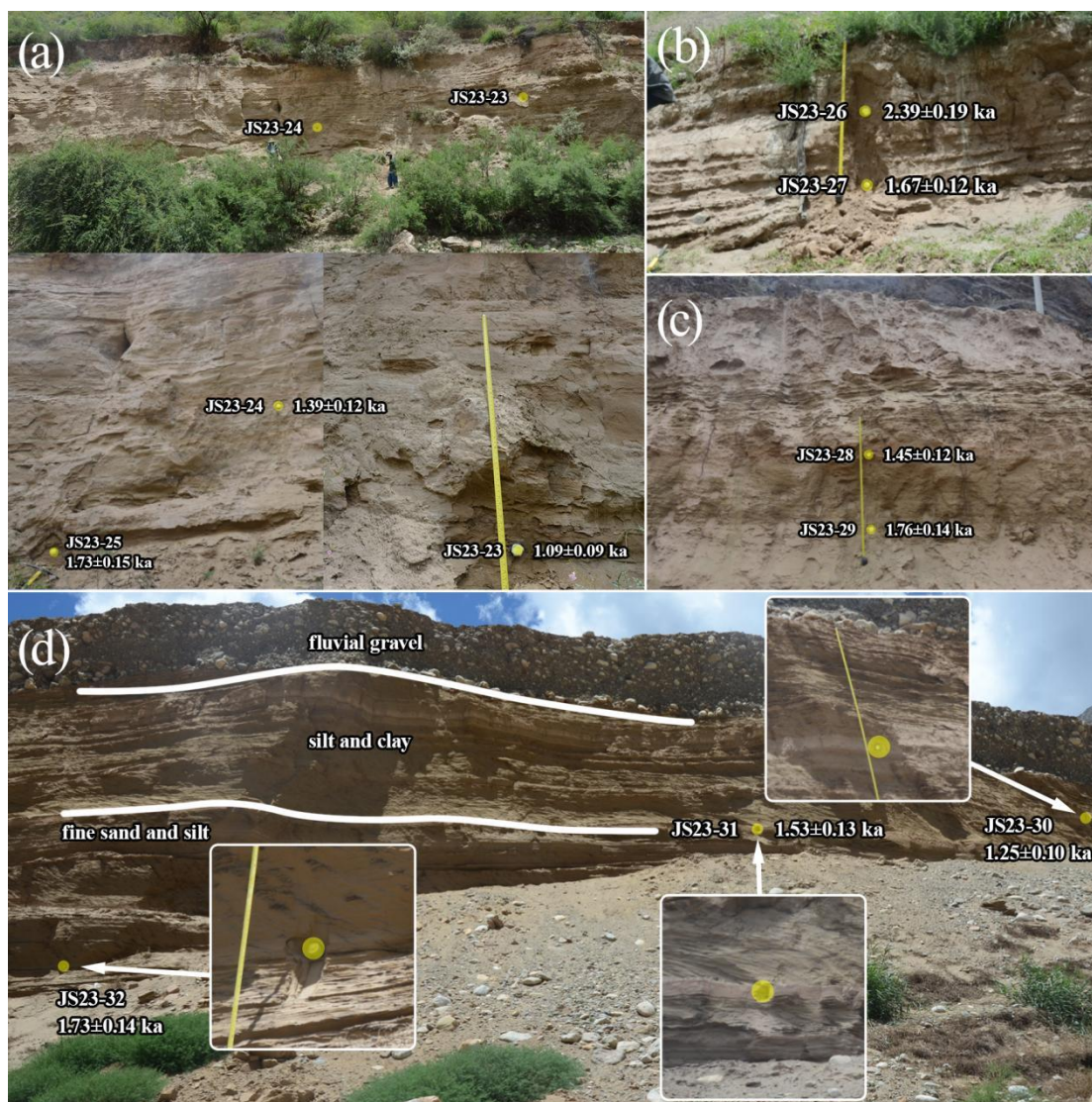


Figure 5 OSL Sample Sections of Lacustrine Sediments

Table 2 Palaeodose, Dose Rate and Ages Obtained from Quartz Extracted from Deposits

Section	Sample ID	Depth (m)	K (%)	Th (ppm)	U (ppm)	Water content (%)	Dose rate(Gy/ka)	No. of aliquotes	Final De (Gy)	OSL Age(ka)
BT-1	JS23-23	7.5	2.244±0.11	9.72±0.49	2.94±0.15	15±5	3.35±0.26	6 ^a +12 ^b	3.65±0.11	1.09±0.09
	JS23-	9.2	1.572±0.08	8.83±0.44	2.55±0.13	15±5	2.62±0.20	6 ^a +12 ^b	3.65±0.14	1.39±0.12

	24									
	JS23-25	10.6	1.342±0.07	7.33±0.37	2.14±0.11	15±5	2.21±0.17	6 ^a +12 ^b	3.82±0.15	1.73±0.15
BT-2	JS23-26	0.6	1.539±0.08	7.65±0.38	2.32±0.12	15±5	2.64±0.19	6 ^a +12 ^b	6.32±0.21	2.39±0.19
	JS23-27	1	1.572±0.08	7.54±0.38	2.30±0.11	15±5	2.68±0.19	6 ^a +12 ^b	4.48±0.08	1.67±0.12
BT-3	JS23-28	3.8	1.587±0.08	8.77±0.44	2.56±0.13	15±5	2.71±0.20	6 ^a +12 ^b	3.93±0.15	1.45±0.12
	JS23-29	4.7	1.339±0.07	6.68±0.33	1.94±0.10	15±5	2.19±0.16	6 ^a +12 ^b	3.85±0.09	1.76±0.14
	JS23-30	5.4	1.637±0.08	8.29±0.41	2.55±0.13	15±5	2.68±0.20	6 ^a +12 ^b	3.35±0.09	1.25±0.10
BT-4	JS23-31	9.2	1.572±0.08	7.87±0.39	2.52±0.13	15±5	2.54±0.19	8 ^a +12 ^b	3.90±0.15	1.53±0.13
	JS23-32	13.1	1.225±0.06	5.73±0.29	1.60±0.08	15±5	1.85±0.14	6 ^a +12 ^b	3.21±0.10	1.73±0.14

^a Aliquot numbers using the SAR protocol; ^b aliquot numbers using the SGC protocol. OD is the overdispersion (%) of De values for each sample.

5 DISCUSSION

5.1 Extent of the Landslide-Dammed Lake

We found a total of 18 lacustrine deposits sections in the study area, and these deposits were all at elevations between 2377 and 2537 m, the elevation of most lacustrine deposits was much lower than the elevation of the nearest landslide dam downstream. Due to the presence of nine landslide dams in the area, we cannot decide which dam these lacustrine deposits were formed. We deduced the original or maximum lake level from the morphology of the relict dam, and the lake area, lake volume and backwater distance are calculated by using 30 m SRTM DEM data. The estimated the peak discharge (Q_p) of the break flood was determined by the formula [27]:

$$Q_p = 0.024 (V)^{0.701} \quad (3)$$

V is lake volume, the outburst flood peak discharge of the nine landslides dammed lake are calculated as below in table 3.

We superimposed the extent of the Wangdalong, Biji, Temi landslide dammed lake on the map (Figure 6), If the lake area is calculated according to lake level 2662 m from the morphology of the relict dam, Its backwater distance is enough to flood the upstream eight paleo landslide dam and all lacustrine deposits (Figure 6a). Therefore, it can be considered that the lacustrine deposits was formed by the Wangdalong landslide dam, the dammed lake duration time is between 1.09-1.76 ka, the lake area is 106.70 million m², the maximum lake volume is 14573.16 million m³, the peak discharge is 31.98×10⁴m³/s.

Table 3 Landslide Dammed Lake Volume and Peak Discharge Statistics

Number	Name	Lake elevation (m)	Dam height (m)	Backwater distance (km)	Lake area (10 ⁶ m ²)	Lake volume (10 ⁶ m ³)	Peak discharge (10 ⁴ m ³ /s)
1	Lawa dammed lake	2585	46	6	1.17	39.31	0.51
2	Temi dammed lake	2645	164	20	6.92	613.8	3.47
3	Niuying dammed lake	2525	46	15	5.05	158.07	1.34
4	Xiaguiwa dammed lake	2535	134	56	26.52	1359.05	6.06
5	Xuelongnang dammed lake	2475	87	18	6.23	319.47	2.20
6	Suoduoxi dammed lake	2469	90	22	8.25	404.24	2.59
7	Suwalong dammed lake	2440	78	14	4.95	183.11	1.49
8	Biji dammed lake	2455	100	34	11.71	628.7	3.53
9	Wangdalong dammed lake	2662	316	107	106.70	14573.16	31.98

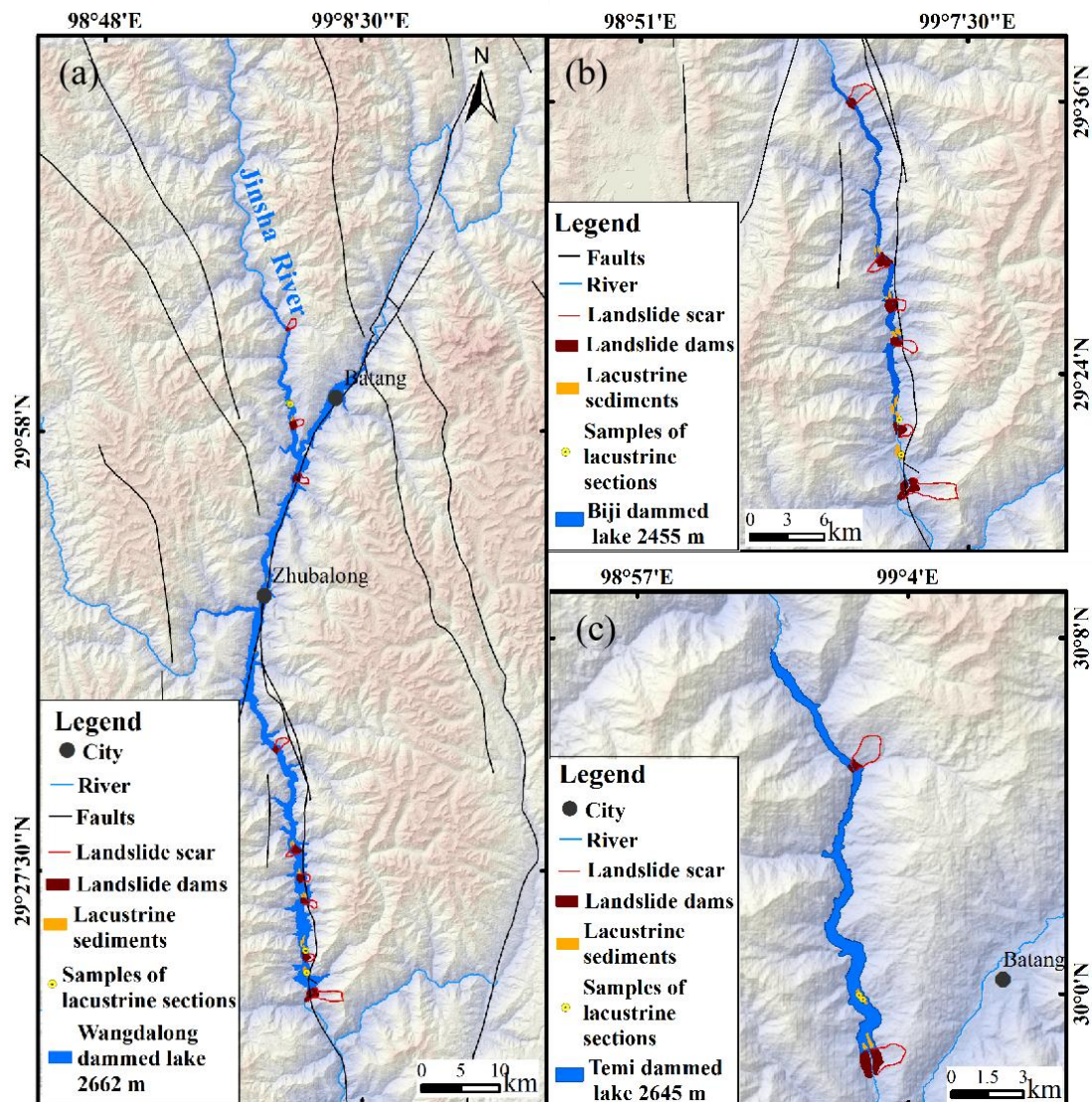


Figure 6 Paleo-Extent of the Wangdalong Dammed Lake. (a) Paleo -Extent of the Wangdalong Dammed Lake Levels of 2662 m a.s.l. (b) Palaeo-Extent of the Biji Dammed Lake Levels of 2455 m a.s.l. (c) Paleo Extent of the Temi dammed Lake Levels of 2645 m a.s.l

Based on optically stimulated luminescence (OSL) dating results of the Temi, Biji, and Wangdalong landslide-dammed lakes, this study reveals that the basal ages of these deposits cluster between 1.7-1.8 ka, demonstrating high chronological consistency. This suggests that these lakes likely formed contemporaneously. Previous studies by Chen et al. (2013, 2018) [11,12] using OSL and ^{14}C dating proposed that at least one major landslide event occurred around 1.9 ka, damming the Jinsha River, with the Xuelongnang landslide dated to ~ 2.1 ka and the Temi landslide to ~ 1.8 ka. Wang et al. (2014) [14] reported that the Wangdalong landslide formed at ~ 1.9 ka, while the Suwalong landslide occurred later (~ 1.36 ka). Integrating these findings, this study posits that the Temi, Biji, and Wangdalong landslides likely occurred between 1.7–1.9 ka. Accounting for dating uncertainties, the formation periods of these dams broadly overlap. The spatiotemporal synchronicity of clustered landslide events strongly implies triggering by a single paleo-earthquake. A similar phenomenon was documented by Brooks [28] in the Quyon Valley (Quebec, Canada), where multiple landslides co-occurred between 980–1060 a and were seismically induced. The Jinsha River Fault Zone (particularly its Batang segment) has historically exhibited intense seismicity, with seven strong earthquakes ($6 \leq M_s \leq 7.5$) recorded since 1722. Numerous paleo-landslide dams along the left bank of the Jinsha River, aligned with the Xionsong-Suwalong active fault, further support a tectonic origin [15]. The study area's two regional active faults—the Jinsha River Fault and Batang Fault—have driven recurrent strong earthquakes. Such tectonic activity progressively weakens rock mass integrity, promoting slope instability. Climatically triggered landslides typically exhibit temporal randomness and spatial dispersion [29], whereas strong earthquakes can induce widespread slope failures within short intervals. Consequently, this study infers that the paleo-landslide dams formed during 1.7–1.9 ka BP were likely seismically triggered under intense tectonic activity.

5.2 Effects of Damming on River Longitudinal Profile

We superimposed the nine landslide dams in the area on the longitudinal section of the Jinsha River according to the

dam volume (Figure 7). We found that the longitudinal profile is steeper where the dams more concentrated, It is especially prominent in the reach of Xuelongnang-Wangdalong. The steepness index (k_{sn}) of the this section river has high values, and form two river knickpoint (kp4 and kp5). However, not all dams have a significant impact on the river profile, the other four landslides (Lawa, Temi, Niuying, Xiaguiwa) does not correspond to the river steepness index high value, this may be related to the landslide of the short duration, a single landslide river less impact on river landscape, and then when they are densely distributed together, the agglomeration effect is not ignore. On the Indus River and the Yarlung River, the longitudinal profile of the river is obviously convex where the dam is gathered, and forms the river knickpoint [10]. Further comparing the slope and width of the upstream and downstream of the dam, we find that the slope of the downstream of the dam becomes higher and the width is relatively smaller, Similar findings have been found in the geomorphic effect of baimakou landslide in Jinsha Rive [7]. Another scholars found that the landslide dam aligns spatially with the elevated sections of the river longitudinal profile and areas exhibiting high k_{sn} values, and coincides with specific river knickpoints in Min, Dadu, Indus and Parlung River [30-32].

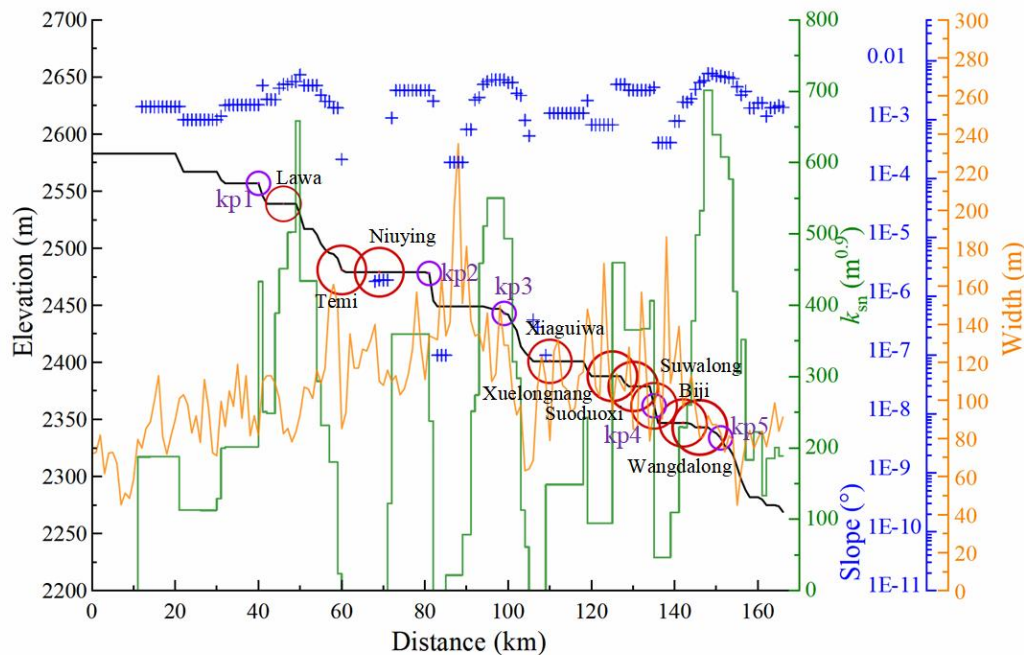


Figure 7 Relationship between Dams, Knickpoints, k_{sn} , Longitudinal Profile, Channel Slope and width of the Jinsha River. River Bed Elevation (Black Line), Knickpoint (Purple Circle), Dam (Red Circle) Log Slope (Blue Cross), Channel Width (Orange Line), k_{sn} (Green Line)

6 CONCLUSION

Through data collection, remote sensing interpretation and field investigation, we found a total of nine landslide dams in the Batang section of the Jinsha River, among which the largest one was Wangdalong landslide dam, the dam height is 316 m, the dam volume is $207.78 \times 10^4 \text{ m}^3$. Further reconstruction of the area landslide dammed lake and OSL dating test, We determined that Wangdalong landslide dam maximum lake surface area reached 106.70 million m^2 , with a maximum volume of 14.57 billion m^3 . The peak discharge flow was calculated at $31.98 \times 10^4 \text{ m}^3/\text{s}$, and the dammed lake existed for a duration of approximately 1.09-1.76 ka. The formation age of this dammed lake is estimated to be between 1.7 ka and 1.9 ka, while the outburst time is between 1.09 ka and 1.25 ka. The dammed lake lasted for approximately 400 to 600 years, and its formation may have been triggered by an earthquake. The densely distributed landslide damming events significantly impact river profiles, making it easier for river knickpoints to form.

COMPETING INTERESTS

The authors have no relevant financial or non-financial interests to disclose.

REFERENCES

- [1] Ouimet W B, Whipple K X, Royden L H, et al. The influence of large landslides on river incision in a transient landscape: Eastern margin of the Tibetan Plateau (Sichuan, China). *Geological Society of America Bulletin*, 2007, 119(11-12): 1462-1476.
- [2] Ouyang C, An H, Zhou S, et al. Insights from the failure and dynamic characteristics of two sequential landslides at Baige village along the Jinsha River, China. *Landslides*, 2019, 16: 1397-1414.

- [3] Ding Y, Zhang X, He Z, et al. Sedimentary environment of a dammed lake buried in the modern riverbed of the Yalong River during the Last Glacial Maximum and its implication for fluvial geomorphic evolution. *Geomorphology*, 2021, 378: 107588.
- [4] Scheingross J S, Limaye A B, McCoy S W, et al. The shaping of erosional landscapes by internal dynamics. *Nature Reviews Earth & Environment*, 2020, 1: 661–676.
- [5] Wang H, Wang B B, Cui P, et al. Disaster effects of climate change in high-Mountain Asia: state of art and scientific challenges. *Advances in Climate Change Research*, 2024, 15(3): 367–389.
- [6] Li Y, Chen J, Zhou F, et al. Identification of ancient river-blocking events and analysis of the mechanisms for the formation of landslide dams in the Suwalong section of the upper Jinsha River, SE Tibetan Plateau. *Geomorphology*, 2020, 368: 107351.
- [7] Liu W, Hu K, Carling P A, et al. The establishment and influence of Baimakou paleo-dam in an upstream reach of the Yangtze River, southeastern margin of the Tibetan Plateau. *Geomorphology*, 2018, 321(15): 167–173.
- [8] Wang H, Wang P, Hu G, et al. An Early Holocene river blockage event on the western boundary of the Namche Barwa Syntaxis, southeastern Tibetan Plateau. *Geomorphology*, 2021, 395: 107990.
- [9] Korup O, Densmore A L, Schlunegger F. The role of landslides in mountain range evolution. *Geomorphology*, 2010a, 120(1–2): 77–90.
- [10] Korup O, Montgomery D R, Hewitt K. Glacier and landslide feedbacks to topographic relief in the Himalayan syntaxes. *Proceedings of the National Academy of Sciences of the United States of America*, 2010b, 107(12): 5317–5322.
- [11] Chen J, Dai F, Lv T, et al. Holocene landslide-dammed lake deposits in the Upper Jinsha River, SE Tibetan Plateau and their ages. *Quaternary International*, 2013, 298: 107–113.
- [12] Chen J, Zhou W, Cui Z, et al. Formation process of a large paleolandslide-dammed lake at Xuelongnang in the upper Jinsha River, SE Tibetan Plateau: constraints from OSL and 14C dating. *Landslides*, 2018, 15(12): 2399–2412.
- [13] Higgitt D L, Zhang X, Liu W, et al. Giant palaeo-landslide dammed the Yangtze river. *Geoscience Letters*, 2014, 1: 1–7.
- [14] Wang P, Chen J, Dai F, et al. Chronology of relict lake deposits around the Suwalong paleolandslide in the upper Jinsha River, SE Tibetan Plateau: Implications to Holocene tectonic perturbations. *Geomorphology*, 2014, 217: 193–203.
- [15] Xia M, Ren G M, Tian F. Mechanism of an ancient river-damming landslide at Batang Hydropower Station, Jinsha River Basin, China. *Landslides*, 2023, 20(10): 2213–2226.
- [16] Larsen I J, Montgomery D R, Korup O. Landslide erosion controlled by hillslope material. *Nature Geoscience*, 2010, 3(4): 247–251.
- [17] Lai Z, Ou X. Basic procedures of optically stimulated luminescence (OSL) dating. *Progress in Geography*, 2013, 32: 683–693.
- [18] Murray A S, Wintle A. Luminescence dating of quartz using an improved single-aliquot regenerative-dose protocol. *Radiation Measurements*, 2000, 32(1): 57–73.
- [19] Liu W, Lai Z, Hu K, et al. Age and extent of a giant glacial-dammed lake at Yarlung Tsangpo gorge in the Tibetan Plateau. *Geomorphology*, 2015, 246: 370–376.
- [20] Lai Z. Testing the use of an OSL standardised growth curve (SGC) for De determination on quartz from the Chinese Loess Plateau. *Radiation Measurements*, 2006, 41(1): 9–16.
- [21] Lai Z, Brückner H. Effects of feldspar contamination on equivalent dose and the shape of growth curve for OSL of silt-sized quartz extracted from Chinese loess. *Geochronometria*, 2008, 30: 49–53.
- [22] Prescott J R, Hutton J T. Cosmic ray contributions to dose rates for luminescence and ESR dating: large depths and long-term time variations. *Radiation Measurements*, 1994, 23(2–3): 497–500.
- [23] Schwanghart W, Scherler D. TopoToolbox 2–MATLAB-based software for topographic analysis and modeling in Earth surface sciences. *Earth Surface Dynamics*, 2014, 2(1): 1–7.
- [24] Whipple K X. Bedrock rivers and the geomorphology of active orogens. *Annual Review of Earth and Planetary Sciences*, 2004, 32(1): 151–185.
- [25] Korup O. Rock-slope failure and the river long profile. *Geology*, 2006, 34(1): 45–48.
- [26] Schwanghart W, Scherler D. Bumps in river profiles: uncertainty assessment and smoothing using quantile regression techniques. *Earth Surface Dynamics*, 2017, 5(4): 821–839.
- [27] Liu W, Carling P A, Hu K, et al. Outburst floods in China: a review. *Earth-Science Reviews*, 2019, 197: 102895.
- [28] Brooks G R. A massive sensitive clay landslide, Quyon Valley, southwestern Quebec, Canada, and evidence for a paleoearthquake triggering mechanism. *Quaternary Research*, 2013, 80(3): 425–434.
- [29] Korup O, Görüm T, Hayakawa Y. Without power? Landslide inventories in the face of climate change. *Earth Surface Processes and Landforms*, 2012, 37(1): 92–99.
- [30] Wang H, Cui P, Liu D, et al. Evolution of a landslide-dammed lake on the southeastern Tibetan Plateau and its influence on river longitudinal profiles. *Geomorphology*, 2019, 343: 15–32.
- [31] Zhou L, Liu W, Chen X, et al. Relationship between dams, knickpoints and the longitudinal profile of the Upper Indus River. *Frontiers in Earth Science*, 2021, 9: 660996.
- [32] Zhou Y, Liu W, Yanites B J, et al. Transient geomorphic response after landslide-induced river damming in the eastern margin of the Tibetan Plateau. *Catena*, 2024, 246: 108386.